Article

The shielding and mechanical properties of Tungsten/epoxy composites

Junxiang Zhang, Shiwei Nie, Shuo Zhang, Tieming Xing, Houhua Xiong*, Zhengkui Zeng*

School of Nuclear Technology and Chemistry & Biology, Hubei Key Laboratory of Radiation Chemistry and Functional Materials, Hubei University of Science and Technology, Xianning 437000

* Correspondence: Correspondence: author: xionghouhua@hbust.edu.cn (H.X.); zengzk@hbust.edu.cn (Z.Z.)

Abstract: With the development of nuclear technology application, radiation safety has been widely concerned, and there is an urgent need for novel shielding materials. Among the various options available, non-lead organic composite shielding material has emerged as a promising solution in the field of radiation shielding due to its high strength, easy processing, and light weight. In this study, tungsten/epoxy resin (W/EP) composite samples with tungsten weight fraction from 0% to 60% were prepared. The shielding and mechanical properties of W/EP composites were investigated. The results show that the results showed that the higher the tungsten content, the greater the shielding capacity of W/EP composites, particularly for low-energy gamma ray (γ) shielding. However, the addition of tungsten reduces the impact strength and tensile properties of the material. Overall, for 300 keV γ-ray, W/EP with 30% tungsten content has comparable shielding capacity to ordinary concrete. W/EP composite materials can serve as shielding materials for low-energy γ-rays.

Keywords: Tungsten; MCNP; Epoxy resin; Gamma rays; shielding

1. Introduction

Nuclear technology is widely used in various fields, such as nuclear power plant, nuclear medicine, nuclear agriculture, industrial irradiation, scientific research, etc.[1]. However, ensuring the safe use of nuclear technology heavily relies on radiation shielding materials. Traditionally, lead bricks, plates, and sheets have been commonly used in radiation shielding materials[2, 3]. Nevertheless, the utilization of lead products has raised concerns over potential harm to human beings. In recent years, researchers have been exploring more environmentally friendly shielding materials with desirable properties like lightness, non-toxicity, high mechanical strength, temperature resistance, and easy processing[4-7].

Non-traditional γ-ray shielding materials, including composites containing tungsten [8, 9], nickel[10], rare earths[11], and metal-organic frameworks (MOFs)[12], have been extensively studied with substrates such as epoxy resin[13], polyethylene[14], rubber[15], polycarbonate[16], and plexiglass[17]. Among the fillers, tungsten has several advantages as a γ-ray shielding material, including its slightly higher shielding capacity compared to lead at the same thickness and its non-toxicity. However, its high melting point, strength, poor plasticity, and toughness make it difficult to process into complex shapes. Mixing tungsten powder or oxide into polymers or easily-formed substrates can solve these problems. Research has been conducted on non-metallic radiation shielding materials with tungsten as a filler, including tungsten with epoxy resin (EP) [18-20], tungsten powder with rubber, tungsten powder mixed with ethylene propylene diene monomer rubber (EPDM) [21], tungsten oxide mixed with concrete[22], tungsten mixed with polyphenylene sulfide (PPS) [23], tungsten powder mixed with polypropylene (PP) [24], tungsten oxide mixed with waterborne polyurethane (WPU) [25], lead and tungsten-doped silicone rubber [26], tungsten with ternary tellurite glass[27], etc. Yan-Zhang et al. [18] prepared and investigated tungsten/epoxy resin composites with heavy tungsten mass fractions,

Preprints (www.preprints.org) | NOT PEER-REVIEWED | Posted: 11 April 2023 doi:10.20944/preprints202304.0205.v1

and found that the shielding capacity of the composite containing 90% tungsten mass fraction was comparable to that of lead. Bashir Ahmed et al. [20] prepared and studied tungsten mixed with silicone resin shielding materials, and discovered that the mass attenuation coefficient of the composite containing 88.1wt% tungsten could reach 0.1035 cm/g. D.K. Gaikwad et al. [27] prepared and investigated tungsten-bismuth-telluride ternary tellurate glass composites, and found that composites containing 20% WO_3 exhibited better shielding capacity than concrete. Hoda Alavian et al. [28] investigated the effect of the size and proportion of tungsten particles on the shielding capacity of low-density polyethylene composites, and found that the mass attenuation coefficient increased with increasing tungsten content. The size effect was more significant at lower tungsten proportions. In general, these results show that the content and size of tungsten or tungsten oxide can significantly affect the shielding capacity and mechanical behavior of tungsten composites. The shielding capacity increased with increasing density of the composite materials, but at the expense of reduced mechanical properties.

Among the matrices, epoxy resin is an engineering plastic that offers excellent mechanical properties and is widely available, easy to process and shape. By adding tungsten powder filler to the epoxy resin matrix, W/PE composites with various complex shapes can be prepared. Move over, W/EP composites are considered environmentally friendly materials. Their mechanical and shielding properties, especially at low tungsten weight fractions, require further investigation. In this study, MCNP5 was used to simulate the shielding properties of W/EP composites. Samples of W/PE composites with different tungsten contents were prepared and evaluated for impact strength, tensile strength, and shielding capacity against γ-rays.

2. Materials and Methods

2.1. Gamma attenuation theory

According to the exponential attenuation law[29, 30], narrow γ-rays pass through shielding materials as expressed in formula (1):

$$I = I_0 e^{-\mu d} \tag{1}$$

where, μ represents the linear attenuation coefficient; I_0 and I denote the initial and attenuated intensities of γ-rays passing through the shielding material, respectively; and d (cm) refers to the thickness of shielding material. As a result, we can derive formula (2) for calculating the linear attenuation coefficient μ (cm) from formula (1):

$$\mu = \frac{Ln(I_0/I)}{d} \tag{2}$$

The shielding properties of materials can also be characterized using other parameters, such as the mass attenuation coefficient μ_m (cm^2/g), half-value layer HVL (cm), and tenth-value layer TVL (cm). The quantity μ_m represents the ability of a substance to shield γ-rays per unit mass thickness, and is related to μ by the formula $\mu_m = \mu/\rho$. The HVL and TVL are defined as the essential thickness to decrease the incoming photon by the factor of half and tenth value, respectively. They can be calculated using the following formulas: $\mathrm{HVL} = \mathrm{Ln}2/\mu$, $\mathrm{TVL} = \mathrm{Ln}10/\mu$.

2.2. Calculation model

A Monte Carlo transport code was employed to calculate the linear attenuation coefficient of shielding materials for narrow γ-rays. The calculation model consisted of a lead chamber, lead collimators, sample, detector, and γ-ray source. The sample was positioned between the source and detector, with the γ-ray source located within the lead chamber. The longitudinal section of the model is illustrated in Figure 1. A tally card (F5 card) was utilized to determine the count at the detector position, with statistical errors of the results less than 2%.

Preprints (www.preprints.org) | NOT PEER-REVIEWED | Posted: 11 April 2023 doi:10.20944/preprints202304.0205.v1

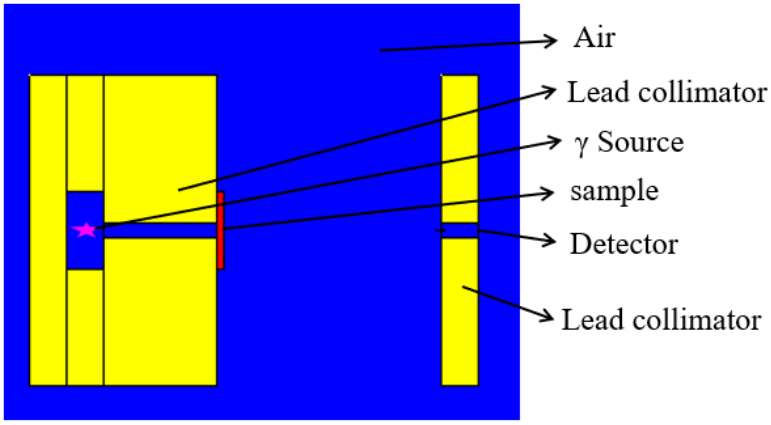

Figure 1. γ Shielding calculation model.

2.3. Experiment

2.2.1. preparation of W/EP Samples

Tungsten powder, with a diameter of 100 nm, was purchased along with epoxy resin (E51), curing agent diethylenetriamine (DETA), acetone, silicone coupling agent, and toughening agent polyether amine D-230. The nano-tungsten powder underwent modification through the addition of a coupling agent. Specifically, 100 g of tungsten powder was mixed with 100 mL of acetone, to which 2g of silicone coupling agent was added. The mixture underwent ultrasonic dispersion and magnetic stirring for 30 minutes each. After allowing the mixture to settle for 10 hours, it was filtered and subsequently dried at 80℃ for 24 hours. As a result, nano-tungsten powder was prepared via surface treatment with a silicon machine coupling agent.

Different tungsten content W/EP samples were prepared by adding 0 g, 2.76 g, 6.20 g, 10.62 g, 16.53 g, 24.8 g and 37.2 g of tungsten powder to 20 g E51, resulting in tungsten weight fractions of 0 wt%, 10 wt%, 20 wt%, 30 wt%, 40 wt%, 50 wt%, and 60 wt%. The mixture was magnetically stirred at 40℃ for 1 hour, followed by the addition of 1.8 g DETA and 3 g D-230. After stirring at room temperature for 30 minutes, the samples were vacuum defrosted, poured into molds, and cured at 40℃ for 15 hours. Four parallel samples were prepared for each composition.

2.2.2. Impact strength and tensile test

The impact strength of the samples was tested using a touch screen-controlled, simply supported beam impact testing machine (ZLCJZL-50), as shown in Figure 2(a). The impact strength test was conducted in accordance with standard GB/T1043.1-2008, "Determination of Impact Properties of Plastic Simply Supported Beams - Part 1: Non-Instrumented Impact Test". The sample size was 80 mm x 10 mm x 4 mm, as depicted in Figure 2(b). The tensile strength and elongation at break of the samples were determined at room temperature using a universal tensile machine (Instron 3369).

Preprints (www.preprints.org) | NOT PEER-REVIEWED | Posted: 11 April 2023 doi:10.20944/preprints202304.0205.v1

Figure 2. (a) Equipment of impact strength test; (b) Samples for impact strength test.

2.2.3γ-. ray shielding properties test

The γ-ray shielding properties were evaluated using a low background multi-channel γ spectrometer, as depicted in Figure 5. Radioactive point sources of ^{137}Cs and ^{60}Co with corresponding γ-ray energies of 662 keV, 1173 keV, and 1332 keV were utilized. The source was contained in a lead cylinder collimator with a 0.5 cm aperture, and the scintillation detector was a NaI(Tl) crystal optically coupled to a phototube. The NaI(Tl) detector had an energy resolution of 8% at 662 keV, and the distance between the source and detector was maintained at 12 cm. The online analysis of the γ-ray spectrum was conducted using Spectrolate Lab version 3.4 computer software, as shown in Figure 3. The attenuation coefficient of the shielding materials was determined by measuring the peak net count with and without shielding materials, denoted as I and I_0 respectively, and calculating according to formula (2).

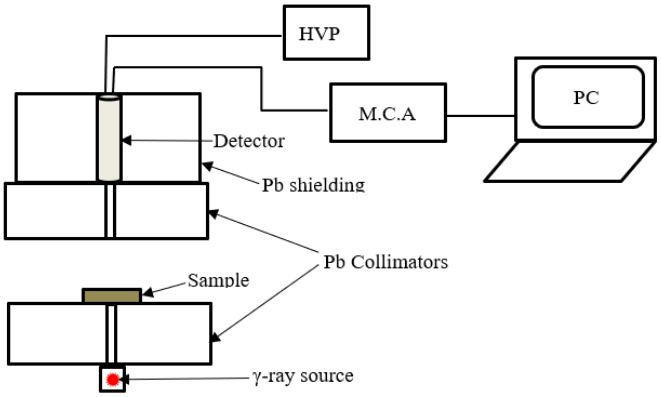

Figure 3. γ-ray shielding properties test system.

3. Results and Discussion

3.1. Impact strength

To analyze the impact strength of the W/EP samples, four parallel samples were tested for each sample with different tungsten content to obtain the average impact strength, and the results are presented in Figure 4. The results indicate that the impact strength of the samples declines with increasing tungsten content. The pure epoxy resin sample exhibits the highest impact strength, measuring 7.81 kJ/cm. When the tungsten fraction rises to 30%, the impact strength decreases by 50.7%, down to 3.85 kJ/cm. Similarly, when the tungsten fraction increases to 60%, the impact strength drops by 52.5% to 3.71 kJ/cm. This reduction can be attributed to the low interfacial force between tungsten and epoxy resin, leading to a decrease in the impact strength of the composites as the tungsten content increases.

Preprints (www.preprints.org) | NOT PEER-REVIEWED | Posted: 11 April 2023 doi:10.20944/preprints202304.0205.v1

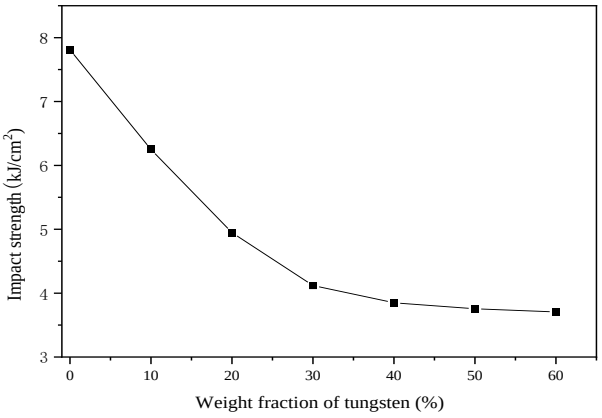

Figure 4. The impact strength varying with tungsten fraction.

3.2. Tensile properties

Samples were subjected to tensile testing at room temperature, and the results of tensile strength and elongation at break are shown in Figure 5. The results reveal that both tensile strength and elongation at break decrease with an increase in tungsten content within the sample. The pure epoxy resin sample displays a tensile strength of 74.3 MPa without adding tungsten powder, while the W/EP sample with 50% tungsten content decreases to 48.4 MPa, indicating a roughly 35% reduction. This suggests that filling epoxy resin with tungsten powder significantly affects the material's toughness, particularly when the tungsten content reaches 40%, as agglomeration becomes more pronounced. Therefore, it is unsuitable to use a large fraction of tungsten in practical applications, as doing so could adversely impact the material's toughness.

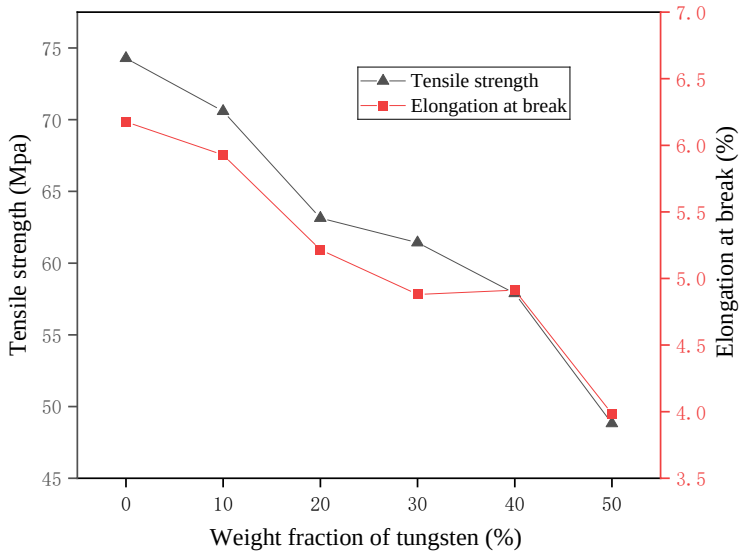

Figure 5. The tensile strength and elongation at break varying with tungsten content.

3.3γ-. ray shielding properties

3.3.1. Verification of calculation

To verify the reliability of the calculation, the linear attenuation coefficient of pure lead (μ_{Pb}) was calculated at different γ-ray energies ranging from 30 keV to 1000 keV. The corresponding results are shown in Figure 6. It can be seen that the linear attenuation coefficient of lead decreases with increasing γ-ray energy, and there is a "weak absorption zone" between 50 and 100 keV. The calculated results are in good agreement with comparison results from literature values [30], indicating the reliability of the calculated results.

Preprints (www.preprints.org) | NOT PEER-REVIEWED | Posted: 11 April 2023 doi:10.20944/preprints202304.0205.v1

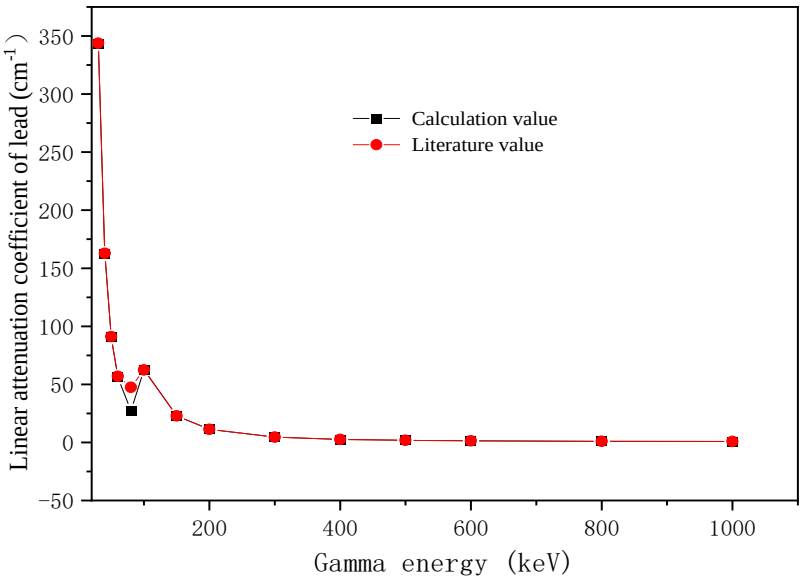

Figure 6. Calculation value and literature value of linear attenuation coefficient of lead.

3.3.2. Linear and mass attenuation coefficient

The linear attenuation coefficient (μ) values of W/EP samples were calculated using MCNP5 and measured using ^{137}Cs (662 keV) and ^{60}Co (1173 and 1330 keV) radiation sources. The linear attenuation coefficient of W/EP samples was calculated by changing the density and nuclide components. The tungsten weight fraction, nuclide components, and density of the W/EP samples are shown in Table 1. The experimental density was obtained using a densitometer, while the theoretical density was calculated using formula (3):

$$\rho_c = \frac{1}{\Sigma_i^n(\omega_i/\rho_i)} \quad (3)$$

where, ω_i and ρ_i *represent* the weight fraction and mass density of the *i* component (filler and matrix) in the composite, respectively. The density of metal tungsten is 19.25g/cm^3, but the density of tungsten powder (nanometer scale) measured by densitometer is about 12g/cm^3. The density of epoxy resin is 1.15g/cm^3, which can be substituted into formula (3) to obtain the density of W/EP composites.

where ω_i and ρ_i represent the weight fraction and mass density of the i component (filler and matrix) in the composite, respectively. The density of metal tungsten is 19.25g/cm^3, but the density of tungsten powder (measured at the nanometer scale) using a densitometer is about 12g/cm^3. To obtain the density of W/EP composites, the density of epoxy resin (1.15 g/cm^3) and tungsten powder (12g/cm^3) was substituted into formula (3).

Table 1. Tungsten wight fraction, nuclides component and density of W/EP composites.

Sample labels	Tungsten fraction (wt%)	Nuclide components				Theoretical density	Experimental density
		C	H	O	W		
0-W/EP	0	0.6875	0.0625	0.25	0	1.15	1.15
1-W/EP	10	0.61875	0.05625	0.225	0.1	1.26	1.25
2-W/EP	20	0.55	0.05	0.2	0.2	1.40	1.32
3-W/EP	30	0.48125	0.04375	0.175	0.3	1.58	1.45
4-W/EP	40	0.4125	0.0375	0.15	0.4	1.80	1.72
5-W/EP	50	0.34375	0.03125	0.125	0.5	2.10	2.04
6-W/EP	60	0.275	0.025	0.1	0.6	2.51	2.38

The linear attenuation coefficient of W/EP composites with different tungsten fraction (0, 10 wt%, 20 wt%, 30 wt%, 40 wt%, 50 wt%, 60 wt%) and ordinary concrete were calculated, and the results are shown in Figure 7 (a)-(b).

Preprints (www.preprints.org) | NOT PEER-REVIEWED | Posted: 11 April 2023 doi:10.20944/preprints202304.0205.v1

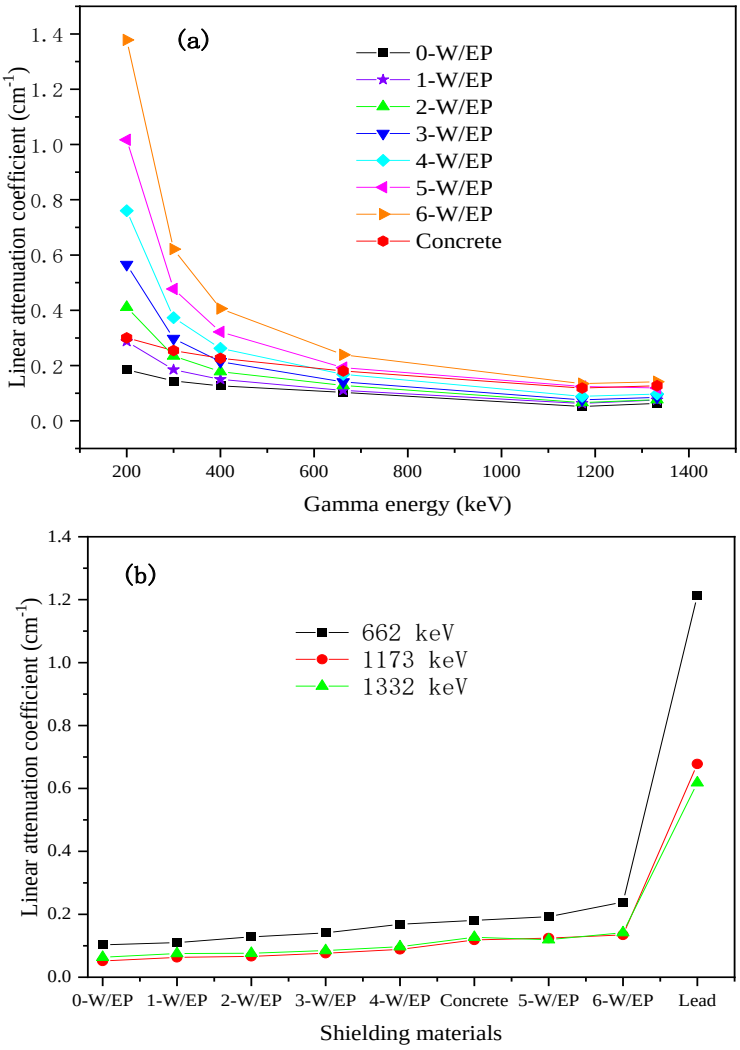

Figure 7. (a) The calculated linear attenuation coefficient of different materials varying with γ-ray energy; (b) The calculated linear attenuation coefficient of different materials at the same γ-ray energy.

The results of Figure 7 (a)-(b) demonstrate that: 1) the linear attenuation coefficient decreases sharply with the increase of γ-ray energy; 2) The linear attenuation coefficient increases with the increase of tungsten content; 3) W/EP composites has more advantages for shielding low energy γ-ray, when γ-ray energy is 200 keV, 300 keV, 400 keV, the shielding capacity of W/EP composites with tungsten fraction of 20 wt%, 30 wt%, 50 wt%, is comparable to that of ordinary concrete; 4) The shielding capacity of W/EP composites with tungsten fraction less than 60 wt% is inferior to that of lead.

Preprints (www.preprints.org) | NOT PEER-REVIEWED | Posted: 11 April 2023 doi:10.20944/preprints202304.0205.v1

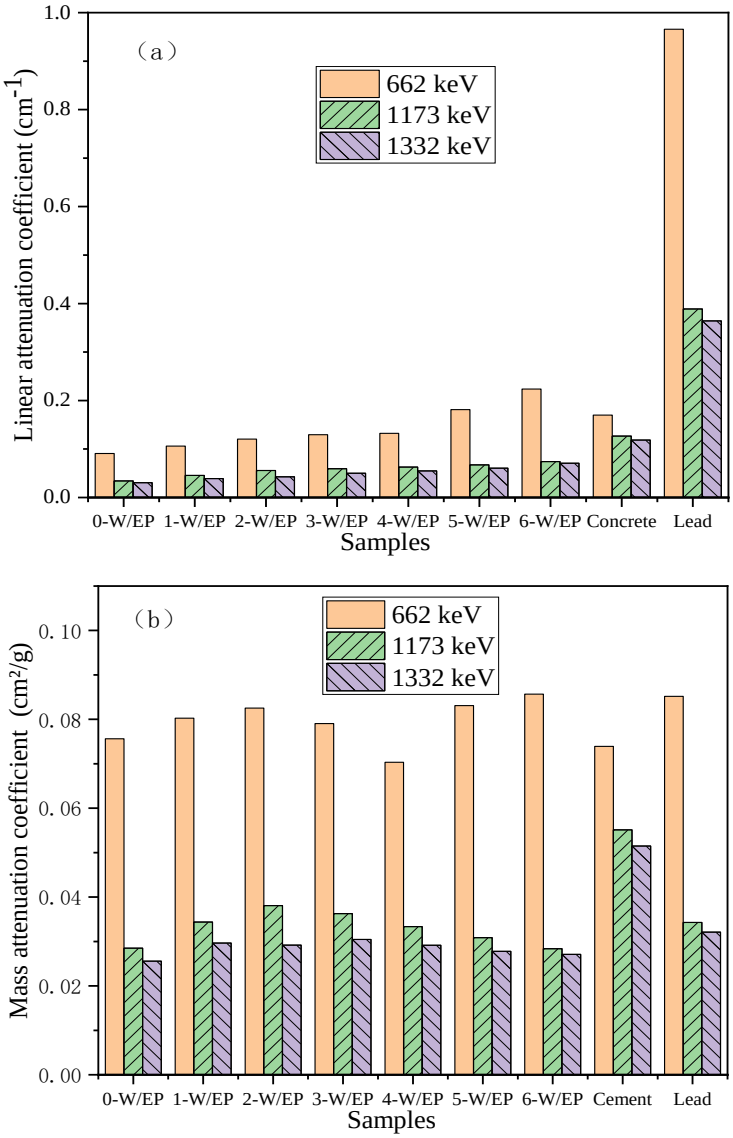

Figure 8. (a) The experimental linear attenuation coefficient of different samples; (b) The experimental mass attenuation coefficient of different samples.

The experimental results of linear and mass attenuation coefficient are shown in Figure 8 (a)-(b), which demonstrate that the experimental values of linear attenuation coefficient of W/EP composites are consistent with the calculated values shown in Figure 7 (b) and Figure 8 (a). but the experimental value is 5-15% lower than the calculated value, which may be caused by the fact that the material density used in calculation is higher than the actual density. Figure 8 (a)-(b) demonstrate that: 1) the linear attenuation coefficient of W/EP samples increases as the tungsten content increases, but remains lower than that of lead. 2) The linear attenuation coefficient of all materials decreases as γ-ray energy increases, indicating the need for thicker shielding material at higher γ-ray energy. 3) For 662 keV γ-ray energy, the shielding capability of 5-W/EP is comparable to that of ordinary concrete; however, for 1173 keV and 1332 keV γ-ray energy, the linear attenuation coefficient of W/EP composites is lower than that of ordinary concrete.

3.3.3. Evaluation of HVL and TVL

According to the theory described in Section 2.1, the HVL and TVL values were calculated and the results are displayed in Figure 9 (a)-(b).

Preprints (www.preprints.org) | NOT PEER-REVIEWED | Posted: 11 April 2023 doi:10.20944/preprints202304.0205.v1

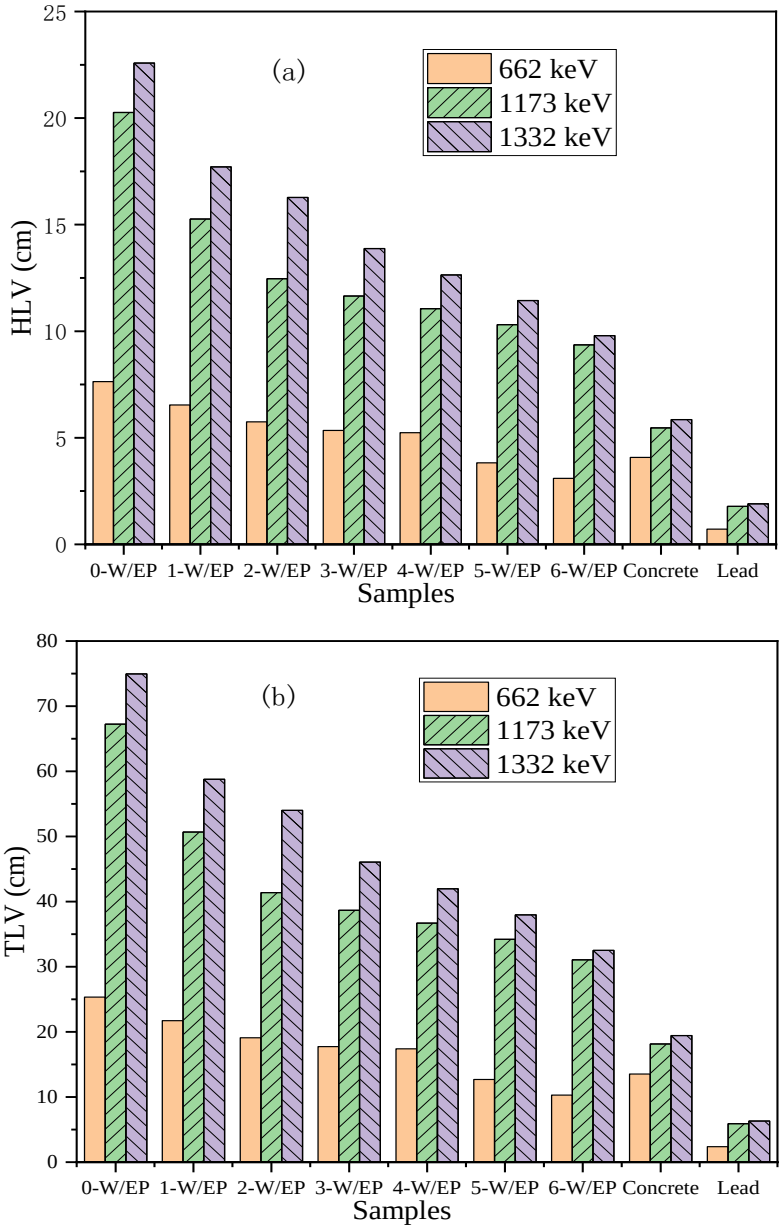

Figure 9. (a) The experimental HVL of different shielding materials; (b) The experimental TVL of different shielding materials.

Based on the results shown in Figure 9 (a)-(b), it can be concluded that the HVL and TVL of W/EP samples decrease with increasing tungsten content, and increase with increasing γ-ray energy. For the high-energy γ-rays of 1773keV and 1332keV, the HVL and TVL of 6-W/EP are greater than those of lead and concrete, indicating that the shielding capability of 6-W/EP composites is slightly worse than that of concrete. However, for the lower energy γ-rays of 662 keV, the HVL and TVL of 5-W/EP are better than those of concrete, but worse than those of pure lead. Specifically, the HVL of 5-W/EP, concrete, and pure lead are 3.82 cm, 4.08 cm, and 0.72 cm, respectively, and the TVL of 5-W/EP, concrete, and pure lead are 12.7 cm, 13.5 cm, and 2.4 cm, respectively. These results suggest that the shielding capability of 5-W/EP is worse than that of pure lead, but better than that of concrete. Moreover, W/EP composites show more advantages in shielding low-energy γ-rays.

4. Conclusions

In this study, the impact strength, tensile properties, and γ-ray shielding properties of W/EP composites were investigated using a combination of MCNP simulation and experiments. Several conclusions were reached, and are as follows:

1. The calculated results indicate that W/EP has comparable shielding capabilities to ordinary concrete at gamma-ray energies of 200 keV, 300 keV, and 400 keV, with tungsten weight fractions of 20%, 30%, and 50%, respectively.
2. The experimental linear attenuation coefficient of W/EP composites is in agreement with the calculated value, but is 5-15% lower than the calculated result.
3. The linear attenuation coefficient of W/EP composites decreases significantly with increasing γ-ray energy, suggesting that thicker shielding materials are necessary to meet the requirements for higher energy γ-ray shielding.
4. The calculated and experimental results reveal that the shielding capability of 6-W/EP composite is slightly inferior to that of concrete for high energy γ-rays with energies of 1773 keV and 1332 keV. Moreover, the shielding capability of 5-W/EP composite is slightly lower than that of pure lead but superior to that of concrete in terms of shielding 662 keV γ-rays. These findings suggest that W/EP composites have more advantages in shielding low-energy γ-rays.
5. The impact strength, tensile strength, and elongation at break of W/EP composites decrease as the tungsten content increases. This is due to a reduction in interfacial force between tungsten and epoxy resin, as well as an increase in tungsten powder agglomeration with higher tungsten content, which leads to a deterioration in mechanical properties. Therefore, it is suggested that excessive addition of tungsten powder should be avoided in practical applications. In summary, an increase in tungsten content results in a decrease of mechanical properties but an increase of gamma-ray shielding capability in W/EP composites, making them more suitable for shielding low energy gamma-rays. The 3-W/EP composite with a 30% tungsten content exhibits comparable shielding capacity to ordinary concrete for 662 keV γ-rays. Additionally, W/EP composites are environmentally friendly and non-toxic materials, indicating their high potential for various applications.

Conceptualization: Hou Xiong and Zheng Zeng; Data curation, Jun Zhang; Formal analysis, Shuo Zhang and Tie Xing; Funding acquisition, Hou Xiong; Investigation, Jun Zhang and Tie Xing; Methodology, Zheng Zeng; Project administration, Hou Xiong; Resources, Hou Xiong; Software, Shi Nie and Shuo Zhang; Supervision, Hou Xiong and Zheng Zeng; Validation, Hou Xiong; Writing – original draft, Jun Zhang and Shi Nie; Writing – review & editing, Hou Xiong and Zheng Zeng. All authors have read and agreed to the published version of the manuscript.

References

1. Angelo, J.A. Nuclear technology. Greenwood Publishing Group, 2004, pp. 443–484.
2. Shultis, J.K.; Faw, R.E. Radiantion Shielding technology. Health Phys. 2005, 88(6):587-612.
3. Mirji, R.; Lobo, B. Radiation shielding materials: A brief review on methods, scope and significance. Proceedings of the National Conference on 'Advances in VLSI and Microelectronics. 2017.
4. More, C.V.; Alsayed, Z.; Badawi, M.S.; Thabet, A.A.; Pawar, P.P. Polymeric composite materials for radiation shielding: A review. Environ. Chem. Lett. 2021, 19: 2057-2090. https://doi.org/10.1007/s10311-021-01189-9.
5. Kharita, M.H.; Yousef. S.; Alnassar, M. Review on the addition of boron compounds to radiation shielding concrete. Prog. nucl. energ. 2011, 53(2):207-211. http://10.1016/j.pnucene.2010.09.012.
6. Chandra, R.J.; Shivamurthy, B.; Kulkarni, S.D.; Kumar, M. S. Hybrid polymer composites for EMI shielding application- A review. Mater. Res. Express. 2019. http://10.1088/2053-1591/aaff00.
7. Alarifi, I.M. Advanced selection in polymer-composite materials for radiation shielding and their properties-A comprehensive review. J. Nucl. Radiat. Sci, 2022, 1(1): 1-1. http://doi.org/10.5455/jnrs.2022.01.001.
8. Kim, S.C. Tungsten-Based Hybrid Composite Shield for Medical Radioisotope Defense. Materials 2022, 15, 1338. https://doi.org/10.3390/ma15041338.
9. Xiao, M.; Qin, Q.; He, X.; Li, F.; Wang, X. Shielding Capability Research on Composite Base Materials in Hybrid Neutron-Gamma Mixed Radiation Fields. Materials 2023, 16, 2084. https://doi.org/ 10.3390/ma16052084
10. Ślosarczyk, A.; Klapiszewski, Ł.; Buchwald, T.; Krawczyk, P.; Kolanowski, Ł.; Lota, G. Carbon Fiber and Nickel Coated Carbon Fiber–Silica Aerogel Nanocomposite as Low-Frequency Microwave Absorbing Materials. Materials 2020, 13, 400.

https://doi.org/10.3390/ma13020400.
11. Jing, H.; Geng, L.Y.; Qiu, S.Y; Zou, H.W; Liang, M.;Deng, D.Research progress of rare earth composite shielding materials. J. Rare. Earth. 2023,Vol.41(1): 32-41. https://doi.org/10.1016/j.jre.2022.06.004
12. Hu, C.; Zhai, Y.T.; Song, L.L.; Mao, X.D. Structure-thermal activity relationship in a novel polymer/MOF-based neutron-shielding material. Polym. Composite. 2020, 41(4): 1418-1427. https://doi.org/10.1002/pc.25465.
13. Sayyed, M.I.; Yasmin, S.; Almousa, N.; Elsafi, M. Shielding Properties of Epoxy Matrix Composites Reinforced with MgO Micro- and Nanoparticles. Materials 2022, 15, 6201. https://doi.org/10.3390/ma15186201.
14. Shin, J.W.; Lee, J.W.; Yu, S.; Baek, B.K.; Hong, J.P.; Seo, Y.; Kim, W.N.; Hong, S.M.; Koo, C.M. Polyethylene/boron-containing composites for radiation shielding. Thermochim. Acta. (2014), http://dx.doi.org/10.1016/j.tca.2014.03.039.
15. Hema, S.; Sambhudevan, S.; Mahitha, P.M.; Sneha, K.; Advaith, P.S.; Sultan, K.R.; Shankar, B. Effect of conducting fillers in natural rubber nanocomposites as effective EMI shielding materials. Mater. Today. https://doi.org/10.1016/j.matpr.2020.01.392.
16. Tang, W.; Lu, L.; Xing, D.; Fang, H.; Liu, Q.; The, K.S. A carbon-fabric/polycarbonate sandwiched film with high tensile and EMI shielding comprehensive properties: An experimental study. Compos. Part B-Eng. 2018, 152: 8-16. http://doi:10.1016/j.compositesb.2018.06.026.
17. Zhang, Y.; Chen, Z.; Zhao, R.; Wang, K.; Wu, D.; Wang, C.; Zhang, M. Insight into the role of free volume in irradiation resistance to discoloration of lead-containing plexiglass. J. Appl. Polym. Sci. 2022, 139(4): 51545. https://doi.org/10.1002/app.51545.
18. Chang, L.; Zhang, Y.; Liu, Y.; Fang, J.; Luan, W.; Yang, X.; Zhang, W. Preparation and characterization of tungsten/epoxy composites for γ-rays radiation shielding. Nucl. Instrum. Meth. B. 2015, 356: 88-93. http://dx.doi.org/10.1016/j.nimb.2015.04.062.
19. Diao, F.Y,; Zhang, Y.; Liu, Y.J.; Fang, J,; Luan, W.L. Preparation and properties of tungsten epoxy resin γ-ray shielding composites. Thermo. Resin, 2016, 31(06):8-12. http://10.13650/j.cnki.rgxsz.2016.06.002.
20. Ahmed, B.; Shah, G.B.; Malik, A.H.; Rizwan, M. Gamma-ray shielding characteristics of flexible silicone tungsten composites. Appl. Radiat. Isotopes. 2020, 155(3):1-13. http://doi:10.1016/j.apradiso.2019.108901
21. Boahen, J.K.; Mohamed, S.A.E.; Khalil, A.S.G.; Hassan, M.A. Finite Element Formulation and Simulation of Gamma Ray Attenuation of Single and Multilayer Materials Using Lead, Tungsten and EPDM. Materials Science Forum. Vol. 1069. Trans Tech Publications Ltd, 2022. https://doi.org/10.4028/p-ol4895.
22. Zalegowski, K.; Piotrowski, T.; Garbacz, A. Influence of Polymer Modification on the Microstructure of Shielding Concrete. Materials 2020, 13, 498. https://doi.org/10.3390/ma13030498.
23. Zhang, Y.; Yang, W.; Zhuang, X.; Liu, J.; Han, J. Study on the properties of PPS composite modified with Tungsten powder, IOP Conference Series: Materials Science and Engineering. IOP Publishing, 2019, 592(1): 012025. http://10.1088/1757-899X/592/1/012025.
24. Liu, C.S.; Yang, G.P.; Liu, Y.; Li, J. Effects of Tungsten content and Particle size on Properties of shielding Composites. Plast. Ind. 2015, 43(05):72-75. http://10.3969/j.issn.1005-5770.2015.05.018.
25. Wu, Z.; Li, Y.; Yan, Q.; Liu, G.; Liu, Y.; Wang, G.; He, L. Gamma radiation shielding properties of WO3/Bi2O3/waterborne polyurethane composites. J. Korean Phys. Soc. 81, 199–205 (2022). https://doi.org/10.1007/s40042-022-00503-0.
26. Dejangah, M.; Ghojavand, M.; Poursalehi, R.; Gholipour, P.R. X-ray attenuation and mechanical properties of tungsten-silicone rubber nanocomposites. Mater. Res. Express. 2019, 6(8): 085045. http://10.1088/2053-1591/ab1a89.
27. Gaikwad, D.K.; Sayyed, M.I.; Botewad, S.N.; Obaid, S.S.; Khattari, Z.Y.; Gawai, U.P.; Pawar, P.P. Physical, structural, optical investigation and shielding features of tungsten bismuth tellurite based glasses. J. Non-Cryst. Solids. 2019, 503: 158-168. https://doi.org/10.1016/j.jnoncrysol.2018.09.038.
28. Alavian, H.; Tavakoli, A.H. Study on gamma shielding polymer composites reinforced with different sizes and proportions of tungsten particles using MCNP code. Prog. Nucl. Energ. 2019, 115(7):91-98. https://doi.org/10.1016/j.pnucene.2019.03.033.
29. Zhu, G.Y.; Chen, H.H. Basis and Application of Ionizing Radiation Protection. Shanghai Jiao Tong University, China, 2016, pp. 50–51.
30. Huo, L.; Liu, J.L.; Ma, Y.H. Radiation dose and Protection. Electronics Industry, Bei jing, China, 2015, pp. 36–37.